



Relationship between shear strength and void ratio of red clay using the fractal model

Yanhao Zheng¹, Kun Shan^{2,*}, Junru Li¹

¹School of Civil and Environmental Engineering, Harbin Institute of Technology (Shenzhen), Shenzhen 518055, China

²PowerChina Huadong Engineering Corporation Limited, Hangzhou 311122, China

*Corresponding author's e-mail: shan_k@hdec.com

Abstract. The strength characteristics of red clay are more complicated than ordinary clay, which directly affects the stability of infrastructure related to red clay. This paper proposes a novel relationship between the shear strength and void ratio of red clay using the existing fractal model to obtain its shear strength more effectively and practically in actual engineering. Through the cooperative analysis of fractal theory and physical properties analysis, the void ratio and shear strength of red clay can be quantitatively described using the fractal dimension. The accuracy of the relationship proposed based on the fractal model is verified by the shear strength of red clay at three stress levels obtained by direct shear tests in the laboratory. As well as proving that the proposed relationship has a good application effect on red clay, the shear test results also show that there is a positive correlation between the shear strength of the remoulded red clay samples and the particle size and the applied normal stress. The research methods and results provide a possible reference and theoretical basis for the application of fractal model to study the mechanical properties of red clay or other types of soil.

Keywords: fractal model; red clay; shear strength; fractal theory; void ratio.

1 Introduction

Red clay, a type of clay with a high liquid limit, is a common soil in south and southwest China, such as Yunnan and Hubei. With the continuous development of China's economy and society, the traffic construction in the red clay region shows a dynamic development [1]. However, red clay has special physical and mechanical properties, which can easily cause roadbed diseases, landslides, and other disasters, seriously affecting the life safety and economic losses of surrounding people [2]. In China, due to red clay slopes and foundations, massive shear failures have occurred in infrastructure [3]. If the foundation soil slippage or partial shear failure extension causes the foundation deformation, the superstructure can't be used normally. The stability of soil around soil slope, retaining wall, and underground structure is affected by soil strength. Therefore, it is very realistic and meaningful to have a clear understanding of the shear strength of red clay.

© The Author(s) 2024

P. Xiang et al. (eds.), *Proceedings of the 2023 5th International Conference on Hydraulic, Civil and Construction Engineering (HCCE 2023)*, Atlantis Highlights in Engineering 26,

https://doi.org/10.2991/978-94-6463-398-6_17

Over the past few decades, many studies have been made on the shear strength of red clay. From the existing literature, it is found that most studies have always explored the shear strength of red clay using the direct shear test [4]. With the development of computer technology and scanning technology, fractal theory has been applied more and more widely. It has also received extensive attention in soil science research [5][6][7]. However, the application of fractal theory in the research of soil mechanical properties is very few. In addition, although the laboratory direct shear test is highly accurate in determining the shear strength of clay, it is difficult to apply to the analysis of large-volume clay samples because of the high time and economic cost of the test, having poor practical application. Therefore, it is necessary to use the fractal model to predict the shear strength of red clay, which is not only economical and practical, but also has a good application effect. For this reason, this study analyses the shear strength of red clay using the fractal theory, expanding the application range of the fractal model.

With the overall aim of proposing a relationship between the shear strength and void ratio of red clay, this study first theoretically analyses the commonly used equations for calculating the shear strength and the fractal characteristics of clay. Then, by modifying the existing fractal model of porous media in rocks and soils, a novel fractal model is proposed to correlate the shear strength of red clay with the void ratio. Based on the results of laboratory tests, the proposed fractal model is verified, and the influence of red clay structure on its mechanical properties is further considered to clarify the relationship between them. The overall idea of the study is illustrated in Figure 1.

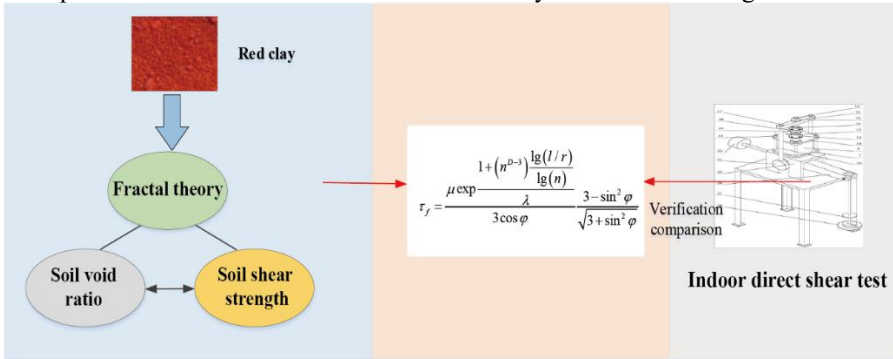


Fig. 1. The general framework of this study

2 Shear strength determination based on fractal model

2.1 Fractal theory

Compared with traditional mathematical and geometric methods, fractal theory is a theoretical method that can ignore the scale of the research object and explain objects with obvious irregularities [8]. Self-similarity and scale invariance are the two most important properties in fractal theory [9]. Self-similarity mainly means that a part of an object can be amplified by a certain factor to characterize its overall attributes [10]. Scale invariance means that no matter how the measurement scale changes, the unique

physical characteristics of the structure, shape, and irregularity of the object will not change [11]. Commonly used fractal dimensions in previous studies include Hausdorff's fractal dimension, box dimension, and capacity dimension [12][13].

2.2 Shear strength analysis based on fractal model

Since the shear strength is affected by the void ratio, there should be a relationship between the void ratio and the shear strength. In this study, the existing fractal model of soil proposed by Tyler et al. [14] was used to explore the relationship model between the void ratio and the shear strength of red clay through theoretical analysis and calculation. However, since this model is only suitable for sandy soil, the Sierpinski gasket and Menger sponge models [15] are introduced to adjust the model to be applicable to red clay. The soil fractal model proposed by Tyler et al. [14] is as follows:

$$M(l \geq L) = \rho_P C_m \left[1 - \left(\frac{L}{\lambda_n} \right)^{3-D} \right] \quad (1)$$

$$M = M(l \geq 0) = \rho_P C_m \left[1 - \left(\frac{L}{\lambda_n} \right)^{3-D} \right] = \rho_P C_m \quad (2)$$

where M represents the cumulative mass distribution; $M(l \geq L)$ represents the total mass of soil particles with a particle size greater than L . λ_n and C_m represents the calculation scale of soil particles and a constant related to particle shape, respectively. M represents the total mass of soil. ρ_P represents the particle density. The maximum sieve opening of soil particles is set to L_{max} . Assuming $l = L_{max}$, the following equation can be obtained.

$$M(l \geq L) = M(l \geq L_{max}) = 0 \quad (3)$$

Equation (4) is calculated by dividing Equation (1) by Equation (2), as shown below:

$$\frac{M(l \geq L)}{M} = \left(\frac{L}{L_m} \right)^{3-D} \quad (4)$$

Then, we can obtain Equation (5):

$$\lg \frac{M(l \geq L)}{M} = (3 - D) \lg \frac{L}{L_m} \quad (5)$$

Since the existing studies have demonstrated that the pore-size distribution of red clay shows obvious self-similarity [16][17], the fractal theory are used to calculate the pore-size distribution of red clay here. First, the initial element shape is set to a cube with a side length of L . In the first iteration, the element shape can be divided into n^3 small cubes, and the side length of each small cube is L/n . In the case of randomly removing m small cubes, $n^3 - m$ cubes are kept. Then, the void ratio of red clay can be derived as follows.

$$e = 1 - \left(\frac{n^3 - m}{n^3} \right) \quad (6)$$

According to Equation (7) proposed by Tyler et al. [14], the functional relationship between fractal dimension D and void ratio e can be expressed by Equation (8).

$$D = \frac{\lg(n^3 - m)}{\lg(n)} \quad (7)$$

$$e = 1 - (n^{D-3})^i \quad (8)$$

In this study, the side length of the initial cube is set to $L=1$, and then the Equation (9) can be obtained. Therefore, the void ratio is converted Equation (10).

$$i = \frac{\lg(L/r)}{\lg(n)} \quad (9)$$

$$e = 1 - (n^{D-3})^{\frac{\lg(L/r)}{\lg(n)}} \quad (10)$$

On the premise of a certain measurement scale, the void ratio can be obtained from the fractal dimension of red clay.

The shear strength of soil can be determined by the following equation (Mitchell and Soga [18])

$$\tau = \mu \sigma_n \quad (11)$$

σ_n is the normal principal stress, τ is the generalized shear stress, and μ is the friction coefficient. As suggested by Mitchell and Soga [18], K_0 , the coefficient of lateral earth pressure, can be written as below.

$$K_0 = 1 - \sin \varphi \quad (12)$$

where φ represents the internal friction angle. According to Mitchell and Soga [18], at the critical state, there is a relationship between τ and σ_n as follows.

$$\tau_f = \frac{\mu \sigma_n}{3 \cos \varphi} \frac{3 - \sin^2 \varphi}{\sqrt{3 + \sin^2 \varphi}} \quad (13)$$

According to the Sierpinski gasket and Menger sponge models [15], as shown in Figure 2, where black corresponds to soil particles, and white corresponds to the pores inside the soil, the soil fractal model proposed by Tyler et al. [14] is optimized. In Figure 2, L represents the size of the particle size, and L_2 represents the overall size of the observation (i.e., the total lateral length). According to fractal theory, the corresponding number of pore networks is calculated as the following equation.

$$N(L) = C \times L^{-D} \quad (14)$$

where C is a random constant. Then, the porosity P can be calculated as follows:

$$P = \frac{C \times L^{2-D}}{L_2^2} = C \times L_2^{-D} \left(\frac{L}{L_2}\right)^{2-D} \quad (15)$$

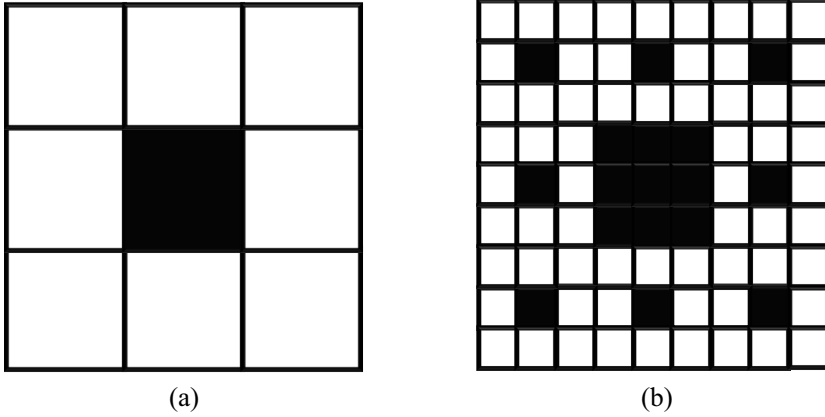


Fig. 2. Sierpinski gasket model (Tyler et al. [14])

In practical applications, L is considered as the particle size or the smallest particle size when the total porosity is calculated. From Figure 2, when observation is made using the observation scale L , only particles with a particle size greater than or equal to L can be detected, and the area must be the total area minus the corresponding pore area, as shown in Equation (16).

$$A(\geq L) = A_a(1 - P) \quad (16)$$

where $A(\geq L)$ represents the total area of particles with a particle size of L or greater, and A_a is the total area of soil within the observation range. Substituting Equation (15) into Equation (16), we can get the equation below.

$$A(\geq L) = A_a[1 - (\frac{L}{L_2})^{2-D}] \quad (17)$$

The same method in the three-dimensional space based on the Menger sponge model [15] is adopted to calculate the volume of soil particles, as shown below.

$$V(\geq L) = V_a[1 - (\frac{L}{L_2})^{3-D}] \quad (18)$$

It is assumed that the scale of observation is granularity R , then Equation (18) can be changed into Equation (19):

$$V(\geq R) = V_a[1 - (\frac{R}{L_2})^{3-D}] \quad (19)$$

where $V(\geq R)$ is the total volume of particles with a particle size of R or larger. V_a is the total volume of soil within the considered range. Equation (19) is completely consistent with the Equation (4) proposed by Tyler et al. [14], indicating that Equation (19) can be used as the fractal model of soil particle volume for red clay.

Combining the results of the above equations, the relationship between the shear strength and the void ratio is obtained, as shown in Equation (20).

$$\tau_f = \frac{\mu \exp^{1+(n^{D-3}) \frac{\lg(l/r)}{\lg(n)}}}{3 \cos \varphi} \frac{\lambda}{\sqrt{3+\sin^2 \varphi}} \quad (20)$$

where λ is the slope of the normal consolidation line.

3 Materials and laboratory experiments

3.1 Source of red clay

The red clay investigated in the present study comes from a construction site in Guiyang, China. The red clay, which is reddish-brown, is collected by drilling at depths of 1-3m below the surface. After sampling, soil samples are first removed from impurities such as branches, leaves, and plant roots, then wrapped in cling film and taken back to a laboratory for testing. Before the test, the collected undisturbed red clay samples are dried, crushed, and screened.

3.2 Physical properties tests and direct shear tests

The reclaimed foundation soil was dried, crushed, and screened (2mm) in accordance with the Soil Testing Procedures (SL237-1999). After using a 0.2 mm fine sieve to screen the soil, the resulting red clay samples were then used for laboratory experiments. The test instruments used here are given in Table 1. The natural water content of red clay was obtained by drying it in an oven. The specific gravity of red clay was measured using the pycnometer method. The liquid limit and plastic limit of red clay were determined by the standard Casagrande method and the manual thread-rolling method, respectively. According to the ASTM D 3080, the standard consolidation fast direct shear tests were performed on remoulded red clay at a constant shear rate under three different consolidation pressures of 100, 200, and 300 kPa.

Table 1. Experimental instruments

Instrument	Model number
Drying oven	RMT-101
Electric Quadruple Equal Strain Direct Shear Apparatus	SDJ-1
Single lever consolidation instrument	WG
Vibrating machine	RX-29-10
Electric relative density meter	A025

4 Results and discussion

4.1 Physical properties analysis

The results of wet density tests suggest that the wet density of the red clay used in this study is always maintained at 1.76-1.81 g/cm³. According to the average wet density of the soil in six experiments, the average dry density is 1.32 g/cm³. The water content of the red clay used in this study is found to be in the range of 35.1%-36.4%. Therefore, we chose the value of 35.7% for further analysis. The specific gravity tests reveal that the final specific gravity of red clay is 2.71, obtained by taking the mean of 6 sets of parallel experiments. For red clay, the natural water content is 35.7%, the liquid limit is 71.26, the plastic limit is 41.35, and the plasticity index and liquidity index are 41.35 and 29.91, respectively, indicating that the red clay investigated in this study is a type of highly plastic clay. Table 2 summarises the obtained data mentioned above.

Table 2. Physical and mechanical properties of red clay.

Project	Numerical value
Dry density (g/cm ³)	1.32
Nature water content (%)	35.7
Liquid limit (%)	71.26
Plastic limit (%)	41.35
Void ratio (<i>e</i>)	1.07
specific gravity (<i>G_s</i>)	2.71

4.2 Fractal dimension characteristics

Figure 3 shows the prediction results of the particle size and porosity of red clay (Figure 3(a)) and the fractal dimension of red clay particles and pores under different dry densities (Figure 3b). The initial dry density of soil is different, and the fractal dimension of particle distribution is different. As the dry density of the soil increases, the fractal dimension of the particles gradually increases. According to the particle packing theory, if the particle distribution is more uniform, the content of secondary particles is too low to effectively fill the pores, resulting in a decrease in compactness and dry density. The greater the unevenness of the particle distribution (the greater the *D*), the more the secondary particle size filled between the coarse particles, the higher the density, the higher the dry density, and the stronger the strength. The fractal dimension of soil pore distribution decreases with the increase of initial dry density. When the soil pores are more uniformly distributed (*D* is small), it will be easily compressed under the action of applied stress, and the pores between the soil are continuously connected, bound, and compressed, thus increasing the dry density of the soil, and increasing the uneven distribution of pores. The resistance between the holes against the applied stress increases, the expansion speed between the pores slows down, the soil becomes larger, and the strength weakens.

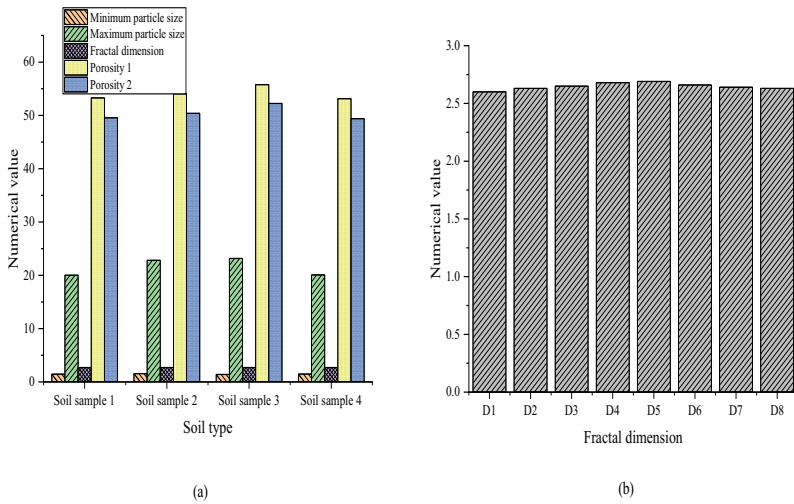


Fig. 3. Prediction results of void ratio (a is the predicted value of void ratio, and b is the fractal dimension of Guiyang red clay in terms of particles and pores under different dry densities.)

4.3 Adoption effect of fractal model

To verify the accuracy of the relationship proposed in this study, the calculation results based on Equation (20) are compared with the results determined by the actual direct shear tests on remoulded red clay, as shown in Figure 4. It is found that the values determined by the proposed relationship are consistent with the actual direct shear test results, suggesting the effectiveness of the proposed equation based on the fractal model proposed in this study. At different stress levels, the minimum difference is 1.41kPa, and the maximum difference is 9.25kPa. The average difference between the results of indoor direct shear tests and the results of the proposed equation based on the fractal model (Equation (20)) is less than 5 kPa, indicating that the relationship proposed based on the fractal model in this study can be used to predict the shear strength of red clay with a good application effect. Not surprisingly, the calculation results from the proposed model show that there is a positive correlation between the shear strength and the applied normal stress, which is consistent with Equation (11) proposed by Mitchell and Soga [18]. But it is also interesting to note that for red clay, the shear strength is proportional to the particle size.

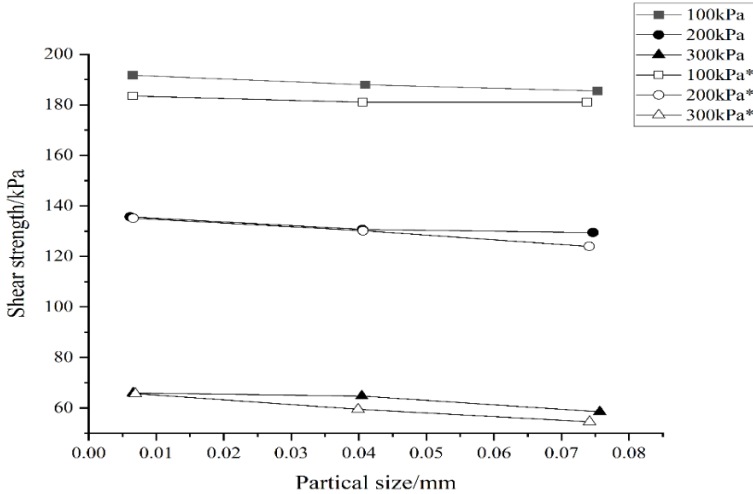


Fig. 4. Comparison of the values of shear strength determined by the relationship proposed based on the fractal model and direct shear testing, where 100kPa, 200kPa, and 300kPa represent the results of the proposed calculation model, while 100kPa*, 200kPa*, and 300kPa* represent the results of the actual direct shear test)

5 Conclusion

In this study, through the cooperative analysis of model theory, a novel relationship between the shear strength and void ratio of red clay was proposed based on the existing fractal model. The physical properties of the studied red clay were first analysed through laboratory experiments. For red clay, on the premise of a certain measurement scale, the void ratio was obtained from the fractal theory, and the shear strength was also quantitatively described by the fractal dimension. Then, a series of indoor direct shear tests were conducted on the remoulded red clay samples at three stress levels. The average difference in the values of shear strength at three different stress levels between the actual direct shear test results and the results determined by the proposed relationship using the fractal model was less than 5 kPa, indicating that the novel relationship proposed in this study can be used to predict the shear strength of red clay with a good application effect. Moreover, the shear test results also suggested that the shear strength of remoulded red clay samples is positively correlated with particle size and applied normal stress. Compared with traditional laboratory direct shear tests, the novel relationship proposed in this study based on the fractal model can not only be used for the accurate and rapid determination of shear strength of large-volume red clay samples but also save time and economic costs, greatly improving the applicability in practical engineering. The methods and results of this study also provide a possible reference for the application of fractal models in the study of red clay or other types of soils. Note that due to the influence of practical factors, this study mainly focuses on a kind of red clay and the research scope will be explored further in the follow-up study.

Acknowledgments

This work was financially supported by the National Natural Science Foundation of China (Grant no: 52239008).

References

1. Y Song, Q Wang, Z An, X Qiang, J Dong, H Chang, ... and X Guo (2018) Mid-Miocene climatic optimum: Clay mineral evidence from the red clay succession, Longzhong Basin, Northern China. *Palaeogeography, Palaeoclimatology, Palaeoecology*, vol. 512, pp. 46-55.
2. S Yang, Z Ding, S Feng, W Jiang, X Huang, and L Guo (2018) A strengthened East Asian Summer Monsoon during Pliocene warmth: Evidence from 'red clay' sediments at Pianguan, northern China. *Journal of Asian Earth Sciences*, vol.155, pp. 124-133.
3. Y Chen, B Li, Y Xu, Y Zhao, and J Xu (2019) Field study on the soil water characteristics of shallow layers on red clay slopes and its application in stability analysis. *Arabian Journal for Science and Engineering*, vol.44, no.5, pp.5107-5116.
4. V H Nhu, N D Hoang, V B Duong, H D Vu, and D T Bui (2020) A hybrid computational intelligence approach for predicting soil shear strength for urban housing construction: a case study at Vinhomes Imperia project, Hai Phong city (Vietnam). *Engineering with Computers*, vol.36, no.2, pp.603-616.
5. E Perfect, and B D Kay (1991) Fractal theory applied to soil aggregation. *Soil Science Society of America Journal*, vol.55, no.6, pp.1552-1558.
6. E Perrier, N Bird, and M Rieu (1999) Generalizing the fractal model of soil structure: The pore-solid fractal approach. *Geoderma*, vol.88, no.3-4, pp.137-164.
7. Y F Xu, and D A Sun (2002) A fractal model for soil pores and its application to determination of water permeability. *Physica A: Statistical Mechanics and its Applications*, vol.316, no.1-4, pp.56-64.
8. F M Mwema, E T Akinlabi, O P Oladijo, O S Fatoba, and S A Akinlabi (2020) Advances in manufacturing analysis: fractal theory in modern manufacturing. *Modern Manufacturing Processes*, vol.2, pp.13-39.
9. Y Deng, M Chen, Y Jin, and D Zou (2016) Theoretical analysis and experimental research on the energy dissipation of rock crushing based on fractal theory. *Journal of Natural Gas Science and Engineering*, vol.33, pp.231-239.
10. J E Hutchinson (1981) Fractals and self similarity. *Indiana University Mathematics Journal*, vol.30, no.5, pp.713-747.
11. H Guo, L Yuan, Y Cheng, K Wang, and Chao Xu (1990) Experimental investigation on coal pore and fracture characteristics based on fractal theory. *Powder Technology*, vol.346, pp.341-349.
12. J Theiler (1990) Estimating fractal dimension. *JOSA A*, vol.7, no.6, pp.1055-1073.
13. S Ikeda (1995) On a fractal set with a gap between its Hausdorff dimension and box dimension. *Hiroshima Mathematical Journal*, vol.25, no.2, pp.433-439.
14. S W Tyler, and S W Wheatcraft (1992) Fractal scaling of soil particle-size distributions: Analysis and limitations. *Soil Science Society of America Journal*, vol.56, no.2, pp.362-369.
15. E Berkove, and D Smith (2020) Geodesics in the Sierpinski Carpet and Menger Sponge. *Fractals*, 28(07), p.2050120.
16. S G Lu, Z Malik, D P Chen, and C F Wu (2014) Porosity and pore size distribution of Ultisols and correlations to soil iron oxides. *Catena*, 123, pp.79-87.

17. L Chen, X Chen, and H Wang (2021) Evolution of the Pore Characteristics of Red Clay Under Axial Strain. *Soil Mechanics and Foundation Engineering*, 58(3), pp.196-202.
18. J K Mitchell, K Soga (2005) Fundamentals of soil behavior (Vol. 3, p. USA). New York: John Wiley & Sons.

Open Access This chapter is licensed under the terms of the Creative Commons Attribution-NonCommercial 4.0 International License (<http://creativecommons.org/licenses/by-nc/4.0/>), which permits any noncommercial use, sharing, adaptation, distribution and reproduction in any medium or format, as long as you give appropriate credit to the original author(s) and the source, provide a link to the Creative Commons license and indicate if changes were made.

The images or other third party material in this chapter are included in the chapter's Creative Commons license, unless indicated otherwise in a credit line to the material. If material is not included in the chapter's Creative Commons license and your intended use is not permitted by statutory regulation or exceeds the permitted use, you will need to obtain permission directly from the copyright holder.

